Journal of
PERIODONTAL RESEARCH

J Periodont Res 2013; 48: 322–330

JOURNAL OF PERIODONTAL RESEARCH
doi:10.1111/jre.12011

p53-Pathway activity and apoptosis in hydrogen sulfide-exposed stem cells separated from human gingival epithelium

B. Calenic[1,2], K. Yaegaki[1], N. Ishkitiev[1], Y. Kumazawa[3], T. Imai[1], T. Tanaka[1]

[1]Department of Oral Health, Nippon Dental University, Tokyo, Japan, [2]Department of Biochemistry, Faculty of Dental Medicine, University of Medicine and Pharmacy "Carol Davila", Bucharest, Romania and [3]Department of Oral Surgery, The Nippon Dental University Hospital, Tokyo, Japan

Calenic B, Yaegaki K, Ishkitiev N, Kumazawa Y, Imai T, Tanaka T. p53-Pathway activity and apoptosis in hydrogen sulfide-exposed stem cells separated from human gingival epithelium. J Periodont Res 2013; 48: 322–330. © 2012 John Wiley & Sons A/S. Published by John Wiley & Sons Ltd

Background and Objective: Hydrogen sulfide (H_2S) is a volatile sulfur compound responsible for physiological halitosis. H_2S was also reported as having periodontal pathologic activities. Gingival crevicular epithelium is the first barrier against periodontal pathogens and their products; oral keratinocyte stem cells OKSCs play key roles in maintaining this barrier. The p53 pathway is responsible for regulating key biological events. Increased apoptosis and cell-cycle arrest of DNA repair can affect keratinocyte stem cells, having a direct impact on the architecture of the oral epithelial tissue. However, the link between H_2S, p53 activity and OKSCs has not yet been fully explored. The main objective of the present study was to explore the implications of the p53 pathway in OKSCs following exposure to H_2S.

Material and Methods: OKSCs were isolated from human gingival epithelium and incubated with physiological levels of H_2S for 24 and 48 h. Apoptosis and the mitochondrial membrane potential were detected using flow cytometry. Cytochrome *c*, total p53, phosphorylated p53 and caspase activity were assessed using specific ELISAs. p53 Pathway gene activity was assayed using quantitative RT-PCR.

Results: The levels of apoptosis were significantly increased following incubation in the presence of H_2S, especially after 48 h (36.95 ± 1.91% vs. 4.77 ± 0.74%). Caspases 9 and 3 were activated, whereas caspase-8 activity remained low. Total p53 activity and particularly phosphorylated p53 at serine 46, were significantly enhanced compared with controls (47.11 ± 9.84 units/mL vs. 1.5 ± 0 units/mL and 32.22 ± 10.23 units/mL vs. 0.15 ± 0 units/mL, respectively, at 48 h). Among p53 pathway genes, apoptosis-related genes [i.e. phosphatase and tensin homolog (*PTEN*), B-cell CLL/lymphoma 2 (*BCL2*), sirtuin 3 (*SIRT3*) and caspases]) were dramatically increased when compared with controls. Moreover, cell-cycle progression genes [i.e. E2F transcription factor (*E2F*) family and histone deacetylase (*HDAC*)] and DNA-repair genes [i.e. growth arrest and DNA-damage-inducible, gamma (*GADD45G*) family and serine/threonine-protein kinase Chk2 (*CHEK2*)] were also increased.

Ken Yaegaki, DDS, PhD, Department of Oral Health, Nippon Dental University, 1-9-20 Fujimi, Chiyoda-ku, Tokyo, 102-8159 Japan
Tel: +81 3 3261 8791
Fax: +81 3 3261 8796
e-mail: yaegaki-k@tky.ndu.ac.jp

Key words: halitosis; hydrogen sulfide; oral epithelia; p53; stem cells

Accepted for publication August 21, 2012

Conclusion: Following incubation with H_2S, OKSCs express multiple p53-associated genes, including programmed cell death, cell-cycle control and DNA-repair genes.

Volatile sulfur compounds (VSCs), mainly composed of in-mouth air, are the only compounds that correlate with oral malodor strength. Among VSCs produced mainly by periodontal pathogens in the oral cavity, particularly those coating the tongue, hydrogen sulfide (H_2S) is the main gas responsible for oral malodor, especially in physiological halitosis, and methyl mercaptan (CH_3SH) is present at a higher level than H_2S in mouth air from periodontal patients (1–5). Previous research reported a strong connection among the development of periodontal disease, periodontal pathogens and H_2S (3,4). Ratkay *et al*. suggested that the effects of VSCs on periodontal tissues are similar to those induced by lipopolysaccharide. Namely, VSCs, such as CH_3SH, can significantly enhance the secretion of prostaglandin E_2, cyclic AMP and procollagenase by human gingival fibroblasts, and also stimulate mononuclear cells to produce interleukin-1, which can increase cyclic AMP production. Moreover, the activity of cathepsin B was also significantly enhanced (6).

H_2S can induce osteoclast differentiation in the alveolar bone (7,8), suppress collagen synthesis and increase collagen degradation (9,10), inhibit the proliferation of oral epithelial (11) and fibroblastic (12) cells, and delay wound healing *in vivo* (9). VSCs also increase the permeability of the basement membrane to prostaglandin E_2 or lipopolysaccharides (13). Moreover, studies on the relationship between apoptosis and periodontitis demonstrate that apoptosis – programmed cell death – plays a critical role in inflammation and in the immune response, contributing to periodontal pathology (5,12–14). We have also described the pro-apoptotic effects of H_2S on oral tissues such as human gingival fibroblasts (14,15), human gingival keratinocytes (16) and osteoblasts (7). Together with the activation of apoptosis, physiological levels of H_2S in the gingival crevice have also been shown to cause oxidative stress, genomic DNA damage and stabilization of tumor suppressor protein p53 in keratinocyte stem cells (14–17). The oral epithelium is the first barrier against microbiological, chemical or physical insults. The integrity of this barrier is highly dependent on the continuous activity of oral keratinocyte stem cells (OKSCs). Tissue homeostasis can therefore be disrupted by dysfunctions in the activity of OKSCs. Cells respond to genotoxic or cellular stress through the p53 signaling pathway (18). p53 regulates a wide variety of biological processes, such as cell-cycle inhibition , growth arrest, DNA repair, senescence or apoptosis (19). Excessive or insufficient activity of these processes can contribute to a wide range of diseases, such as cancer, degenerative disorders or viral infections (20).

In a previous study we showed that p53 is activated and initiates mitochondrial apoptosis in keratinocyte stem cells (17). However, owing to the unavailability of OKSCs, we utilized a keratinocyte stem-cell line originated from human skin. Therefore, we have recently managed to isolate a novel population of OKSCs from human gingiva (21). Stem cells were separated using a magnetic separation technique and two markers – integrin $\alpha_6\beta_4$ (expressed only on basal keratinocytes) and CD71 (a proliferation-related marker). Cells with the $\alpha_6\beta_4^{pos}$ $CD71^{neg}$ phenotype were characterized as OKSCs (21). The previous study focused only on the apoptotic process (17). Moreover, the p53 pathway activity following exposure of OKSCs to H_2S has not yet been fully understood. The specific aim of the present study was to explore the extensive molecular mechanisms underlying p53 pathway activation following exposure of a population of OKSCs, separated from human gingival epithelium, to H_2S.

Material and methods

Separation and culture of OKSCs

All protocols were approved by the Research Ethics Committee of Nippon Dental University. Gingival tissues were supplied by patients undergoing oral surgery at Nippon Dental University Hospital. Informed consent was obtained from all patients involved in the study. The cells used in the experiments were human OKSCs separated from human gingival epithelium using a protocol developed in our laboratory (21). Tissues were subjected to enzymatic dissociation in 3 mg/mL of collagenase (Sigma, St Louis, MO, USA) and 4 mg/mL of Dispase II (Sigma) for 24 h at 4°C. After treatment, the epidermis and the connective tissue were separated. To obtain viable single keratinocyte cells, the epithelial sheets were treated with 0.05% trypsin (Sigma) for 30 min at 37°C. OKSCs were magnetically separated using two markers – integrin-$\alpha_6\beta_4$ [mouse monoclonal (450-30A) antibody to Integrin alpha 6 beta 4; Abcam®, Tokyo, Japan] and a proliferation-related marker, CD71 (MicroBeads conjugated to monoclonal mouse anti-human CD71 IgG2a; Miltenyi Biotec Inc., Auburn, CA, USA) – and a MACS® Separator (Miltenyi Biotec Inc.). For magnetic separation the cells were incubated with $\alpha_6\beta_4$-fluorescein isothiocyanate-conjugated antibody (Abcam). The cells were further reacted with goat anti-mouse IgG MicroBeads (Miltenyi Biotec Inc.), then the cell suspension was loaded onto a column placed in the magnetic field. The magnetically labeled cells were retained in the column – $\alpha_6\beta_4^{pos}$ cell fraction – while

the unlabeled cells ran through the column (the $\alpha_6\beta_4^{neg}$ fraction). Further $\alpha_6\beta_4^{pos}$ cell fraction was magnetically labeled with CD71 MicroBeads. The labeled CD71 cells were retained in the column, while the unlabeled CD71 cells ran through the column. After both separations the total number of cells was divided into three fractions: $\alpha_6\beta_4^{neg}$ (normal keratinocytes); $\alpha_6\beta_4^{pos}$ $CD71^{pos}$ (transit-amplifying cells); and $\alpha_6\beta_4^{pos}$ $CD71^{neg}$ (OKSCs). The cells with the $\alpha_6\beta_4^{pos}$ $CD71^{neg}$ phenotype were used in the H_2S experiments.

For each experiment the cells were cultured in 35-mm-diameter dishes precoated with human collagen type IV (20 μg/mL) (Sigma) at 36°C in an atmosphere of 5% CO_2 at 2×10^5 cells/dish and were allowed to attach overnight. Before exposure to H_2S, the cells were washed with phosphate-buffered saline and then placed in fresh medium. The medium used was EpiLife® Defined Growth Supplement (EDGS) (Cascade Biologics, Portland, OR, USA) supplemented with 0.25 μg/mL of Fungizone and 0.250 mg/mL of kanamycin. The samples were placed in an H_2S incubation system and incubated in 50 ng/mL of H_2S mixed with 5% CO_2 in air for 24 and 48 h for apoptosis detection and for 48 h for apoptotic pathway analysis. In the medium, as a result of diffusion, H_2S concentration was found to be 0.5 μM, a much lower concentration than that found in gingival crevicular fluids from periodontal gingival tissues (5). Negative-control samples were incubated in CO_2 without H_2S.

The H_2S incubation system consists of an H_2S permeator (PD-1B-2; Gastec, Kanagawa, Japan) and H_2S permeation tubes (Permeacal; Gastec) and has been fully described previousslt work (14–17).

Flow cytometry

Flow cytometry was used to detect apoptosis and mitochondrial membrane potential, as described later. Data acquisition was performed using the Guava EasyCyte (Guava Technologies, Hayward, CA, USA) flow cytometer. Data analysis was performed using Guava CytoSoft software.

Apoptosis detection

Early apoptosis and late apoptosis which contains necrotic cells too were detected using an apoptosis kit (Guava Nexin PCA; Guava Technologies). The method of detection is based on two fluorescent dyes – 7-aminoactinomycin D (7-AAD) and Annexin V-phycoerythrin conjugate (Annexin V-PE) – allowing direct detection and quantification via flow cytometry. Each experiment was performed using 1×10^3 OKSCs.

Mitochondrial membrane potential

Membrane depolarization was analyzed by measuring the uptake, into the mitochondria, of a cationic dye, 5,5′,6,6′-tetrachloro-1,1′,3,3′-tetraethylbenzamidazolocarbocyanin iodide, also known as JC-1. 7-AAD was used to detect late apoptotic and necrotic cells. Following incubation with H_2S, the cells were incubated with 2 μL of JC-1 and 2 μL of 7-AAD for 30 min and then analyzed by flow cytometry.

ELISA detection

A quantitative sandwich enzyme immunoassay technique was employed for cytochrome *c*, caspases 8, 9 and 3, total p53 and phosphorylated p53. The following kits were used: Cytochrome C ELISA (Calbiochem, Darmstadt, Germany) for cytochrome *c*; Human caspase-8 ELISA Quantikine™ (R&D Systems, Minneapolis, MN, USA) for caspase-8; Human caspase-9 ELISA Quantikine™ (R&D Systems), for caspase-9; Human active caspase-3 ELISA Quantikine™ (R&D Systems) for caspase-3; Total p53 ELISA kit (Cyclex Co., Nagano, Japan) for total p53; and Phospo-p53 Ser 46 ELISA kit, (CycLex Co.) for phosphorylated p53. Samples, controls and standards were pipetted into wells precoated with a monoclonal antibody specific for each marker. Following a washing step, substrate solution was added to the wells. After another washing step, an enzyme-linked monoclonal antibody specific for each assay was added to all wells. The absorbance was determined using a microplate reader (Bio-Rad Benchmark Plus; Bio-Rad, Tokyo, Japan) set to specific wavelengths.

Real-time RT-PCR analysis

For analyzing p53 signaling-associated genes we used a TaqMan® Array Human p53 Signaling, Fast 96-well Plate (Applied Biosystems, Foster City, CA, USA). The plate contains genes related to the p53 pathway with key roles in cell-cycle control and DNA damage and repair, the apoptotic process and cell senescence, as well as signal transduction molecules and transcription factors. The protocol followed the manufacturer's instructions. Briefly, the first step was to use a reverse-transcription reaction to obtain complementary DNA from total RNA. The next step was the reconstitution of the array plate using 10 μL of master mix and the complementary DNA sample. The plates were run on a real-time PCR system (StepOnePlus Real-Time PCR System; Applied Biosystems) that allows the quantification of RNA-expression levels.

Statistical analysis

The results from five independent experiments are presented as mean ± standard deviation. Statistical analysis was performed using one-way analysis of variance. Statistical significance was accepted at $p < 0.05$. The levels of the relative quantification were calculated using the $2^{-\Delta\Delta C_t}$ method by the real-time PCR system mentioned above (22).

Results

H_2S-induced apoptosis

The results obtained using the Guava EasyCyte results flow cytometer were analyzed using Guava CytoSoft software. Early apoptotic cells were clearly separated, as reported previously (23). The number of early

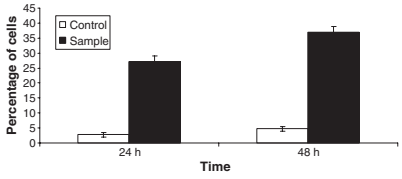

Fig 1. Hydrogen sulfide (H_2S) triggers apoptosis in human oral keratinocyte stem cells isolated from the gingival epithelium. After both 24 and 48 h, a significant difference was found between samples and their corresponding controls. Each data point represents mean ± standard deviation of six independent experiments ($p < 0.05$ vs. control).

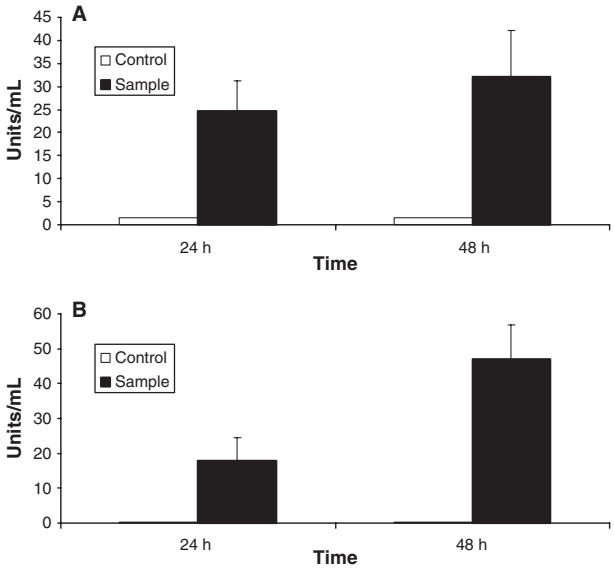

Fig 2. p53 Activity. (A) Total p53 activity following incubation of oral keratinocyte stem cells (OKSCs) in hydrogen sulfide (H_2S). Total p53 includes phosphorylated p53. (B) Phosphorylated p53 activity following incubation of OKSCs in (H_2S). Each data point represents mean ± standard deviation of six independent experiments ($p < 0.05$ vs. control).

apoptotic cells was significantly increased, in a time-dependent manner, after both 24 and 48 h of incubation when compared with their control groups (27.13 ± 1.88% vs. 2.79 ± 0.72% after 24 h of incubation and 36.95 ± 1.91% vs. 4.77 ± 0.74% at 48 h of incubation) ($p < 0.05$, respectively, $n = 6$) (Fig. 1). At each time point, late apoptotic and necrotic events were found to be < 5%, and no difference was found between the control and test groups at any time point.

Total p53 and phosphorylated p53

At each time point total levels of p53 which is tumor suppressor limits cellular proliferation by inducing cell-cycle arrest and apoptosis in response to cellular stresses such as DNA damage, were significantly increased compared to their respective controls (16–18) (24.69 ± 6.45 units/mL vs. 1.5 ± 0 units/mL at 24 h and 47.11 ± 9.84 units/mL vs. 1.5 ± 0 units/mL at 48 h) ($p < 0.05$, $n = 6$) (Fig. 2A). Phosphorylated p53 at serine 46, which plays a critical role in p53-mediated apoptosis, was also increased after both 24 and 48 h (18.02 ± 4.26 units/mL vs. 0.15 ± 0 units/mL at 24 h and 32.22 ± 10.23 units/mL vs. 0.15 ± 0 units/mL at 48 h) ($p < 0.05$, $n = 6$) (Fig. 2B).

Cytochrome *c* and mitochondrial membrane potential detection

Depolarized mitochondrial membrane causes the release of cytochrome *c*, which activates the caspase cascade (14–17). The number of membrane-depolarized cells was significantly increased at each time point compared with controls (28.53 ± 3.85% vs. 5.78 ± 1.08% at 24 h and 48.18 ± 10.22% vs. 6.08 ± 2.89% at 48 h) ($p < 0.01$, $n = 6$). A significant increase of cytochrome *c* in the cytosol was also observed (0.26 ± 0.01 ng/mL vs. 0.18 ± 0.01 ng/mL at 24 h and 0.46 ± 0.05 ng/mL vs. 0.18 ± 0.01 ng/mL at 48 h) ($p < 0.05$, $n = 6$).

Caspase activities

After incubation in H_2S, caspase-3, executer enzyme of apoptosis, was significantly activated compared with controls (14–17) (0.75 ± 0.19 ng/mL vs. 0.20 ± 0.01 ng/mL at 24 h and 1.22 ± 0.23 ng/mL vs. 0.22 ± 0.23 ng/mL at 48 h) ($p < 0.05$, $n = 6$). Significant differences were also found between caspase-9 activity, which activates caspase-3, in test groups compared with their controls (6 .20 ± 1.19 ng/mL vs. 1.36 ± 0.59 ng/mL at 24 h and 12.53 ± 0.83 ng/mL vs. 1.36 ± 0.59 ng/mL at 48 h) ($p < 0.01$, $n = 6$). On the contrary, caspase-8 levels remained low and comparable with those in control groups (0.18 ± 0.05 ng/mL vs. 0.24 ± 0.01 ng/mL at 24 h and 0.14 ± 0.04 ng/mL vs. 0.24 ± 0.04 ng/mL at 48 h) ($n = 6$) (Table 1).

p53 Pathway

Multiple p53 pathway genes were increased by sevenfold or higher following 48 h of incubation in H_2S. For each gene the results were expressed as relative fold-change compared with their respective controls. The relative fold-changes of apoptosis-related genes were as follows: phosphatase and tensin homolog (*PTEN*), 7.90 ± 0.04; B-cell CLL/lymphoma 2 (*BCL2*), 8.09 ± 0.32; sirtuin 3 (*SIRT3*), 7.77 ± 1.94; caspase 3 (*CASP3*), 14.04 ± 1.09; caspase 4 (*CASP4*), 7.35 ± 1.52; caspase 7 (*CASP7*), 8.87 ± 1.47; caspase 6 (*CASP6*), 7.75 ± 1.07; and histone deacetylase 5 (*HDAC5*), 7.17 ± 0.33 ($n = 3$) (Fig. 3A). The relative fold-changes of cell-cycle progression genes were as follows: E2F transcription factor 6 (*E2F6*), 7.07 ± 0.93; E2F transcription factor 2 (*E2F2*), 30.09 ± 1.61; E2F transcription factor 4 (*E2F4*), 14.90 ± 0.82; and histone deacetylase 4 (*HDAC4*), 7.33 ± 0.78 ($n = 3$) (Fig. 3B). The relative fold-changes of

Table 1. Caspase activities at 48 h of incubation with hydrogen sulfide (H_2S)

	Caspase-9	Caspase-8	Caspase-3
Control	1.36 ± 0.59	0.24 ± 0.04	0.22 ± 0.23
Sample	12.53 ± 0.83	0.14 ± 0.04	1.22 ± 0.23

All caspase activities are expressed in ng/mL. Caspase-8 activity remained low, proving the inactivity of the extrinsic apoptotic pathway. Caspase-9 and -3 levels were significantly increased, suggesting that H_2S-induced apoptosis is activated via an intrinsic apoptotic pathway. Each data point represents the mean ± standard deviation of six independent experiments ($p < 0.05$ vs. control).

DNA-repair genes were as follows: growth arrest and DNA-damage-inducible, gamma (*GADD45G*), 62.69 ± 2.26; growth arrest and DNA-damage-inducible, alpha (*GADD45A*), 17.03 ± 1.27; growth arrest and DNA-damage-inducible, beta (*GADD45B*), 8.92 ± 0.98; checkpoint kinase 2 (*CHEK2*), 7.14 ± 1.10; and sirtuin 6 (*SIRT6*), 8.89 ± 0.98 ($n = 3$) (Fig. 3C).

Discussion

Depending on cell type, apoptosis is activated through the intrinsic-mitochondrial pathway or the extrinsic cell-death ligand pathway: p53 plays an important role in both pathways. Regardless of the type of stress upon p53 activation, the cells respond with a wide range of biological processes, ultimately leading to cell-cycle arrest followed either by DNA repair or by apoptosis (24,25). In our previous studies we have identified the expression of p53 pathway genes that are involved in the apoptotic process, the inhibition of cell-cycle progression, DNA repair or senescence (17). A cell's fate can be decided by specific phosphorylation of p53 (26). Phosphorylation at serine 46 activates p53-dependent apoptosis following severe DNA damage (27). Physiological levels of H_2S inhibit superoxide dismutase (14). Inhibition of superoxide dismutase activity causes critical accumulation of reactive oxygen species, which translates into cellular oxidative stress. Moreover, H_2S is recognized to be a decisive inhibitor of cytochrome *c* oxidase, which is a key enzyme for oxidative phosphorylation in the respiratory chain of the mitochondria to produce adenosine triphosphate (27–29). Consequently, a large amount of reactive oxygen species are produced (30,31). Oxidative stress can damage cellular biomolecules, including DNA, which in turn stabilizes p53. In human gingival tissues, H_2S produces a large number of DNA double-strand breaks (14–17). The present study demonstrated that after 48 h of incubation in H_2S there was a significant increase in both the total levels of p53 and serine 46 phosphorylated-p53. As p53 is an important activator of major apoptotic pathways, apoptotic levels were significantly increased when compared with respective controls, as determined by flow cytometry. To distinguish between the two apoptotic pathways we analyzed key markers from both pathways using ELISAs. For the intrinsic pathway we analyzed mitochondrial changes and the activity of initiator caspases that are involved in the mitochondrial pathway. After 48 h of incubation with H_2S, the mitochondrial membrane potential had collapsed. Disruption of the electrochemical gradient is crucial for the release of cytochrome *c* from the inner mitochondrial membrane into the cytosol (32). It was also shown that there was a significant release of cytochrome *c* into the cytosol. Cytochrome *c* triggers the formation of the apoptosome, which in turn recruits and activates initiator caspase-9 (33). In this study, OKSCs exposed to H_2S showed a significant increase in caspase-9 activity. At the same time, caspase-8 was not activated, suggesting that the extrinsic cell-death ligand pathway is not involved in the apoptotic process; moreover, cytotoxic T-cell-mediated apoptosis was excluded from this study (34).

Expression of the gene encoding the executioner caspase-3 was 15-fold higher in OKSCs exposed to H_2S than in the control group, providing further evidence to support the fact that the mitochondrial intrinsic pathway is responsible for H_2S-induced apoptosis. Our PCR data also showed that besides caspase-3, other downstream caspases (caspases 6 and 7) are also involved. The caspase 6 gene, which is activated in the cytochrome *c*-induced pathway, was increased sevenfold more than in controls. Aside the executioner role in apoptosis, caspase-6 is also responsible for keratin cleavage during apoptosis in epithelial cells (35). Caspase-6 may therefore be involved in the disruption of the cytoskeleton in OKSCs during the apoptotic process. Caspase-7 activity was also significantly increased. It has been shown that caspase-7, together with caspase-3, is a key mediator of the mitochondrial events of apoptosis (36). In addition to its role as a downstream caspase in the intrinsic pathway, caspase-7 participates in cytochrome *c* release and is an apoptosis-inducing factor. Caspase-4 is an inflammatory caspase member of the caspase-1 family found in endoplasmic reticulum (37). Recent research demonstrates that caspase-4 is mainly activated in endoplasmic reticulum-stress induced apoptosis (38). In our study, H_2S also significantly increased the expression of the caspase 4 gene compared with controls, suggesting that other pathways, such as the caspase-4 pathway, may also be implicated in the apoptotic process in gingival keratinocyte stem cells as well as in p53 activation.

p53 Phosphorylation and stabilization is mediated by a DNA checkpoint protein, checkpoints factor-2 (Chek2) (39). In our experiments, the *Chek2* gene was expressed at a significantly higher level compared with specific controls. Data on p53 obtained from this study showed that from total p53, only two-thirds was phosphorylated at serine 46, suggesting that p53 activation is involved not only in the apoptotic process but also in other processes (e.g. cell-cycle progression) (26). This implication is also

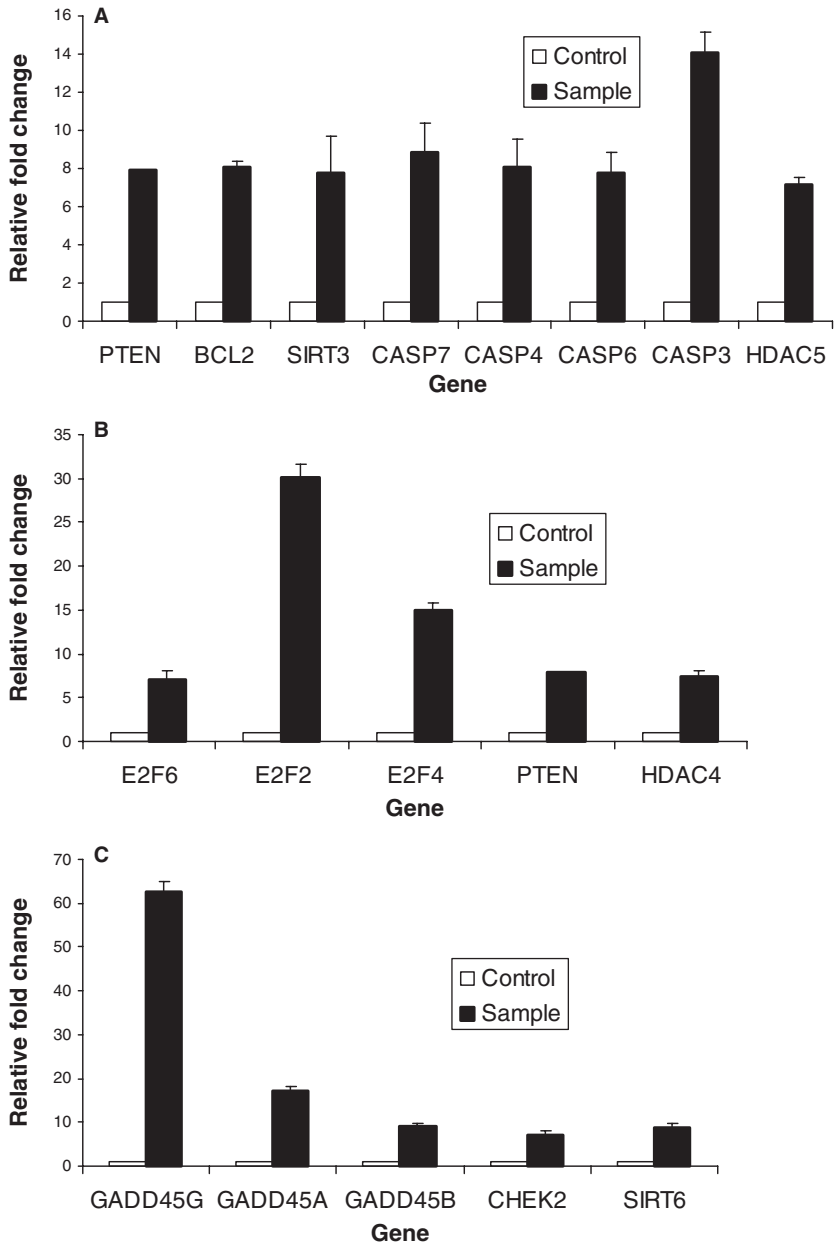

Fig 3. p53 Pathway gene activity. (A) Apoptotic genes activated as a result of 48 h of exposure to hydrogen sulfide (H_2S). (B) Cell-cycle progression genes in oral keratinocyte stem cells activated by H_2S; (C) DNA-repair genes activated as a result of the genotoxic effect of H_2S. Data are given as mean and standard deviation of three independent experiments. *BCL2*, B-cell CLL/lymphoma 2; *CASP3*, caspase 3; *CASP4*, caspase 4; *CASP6*, caspase 6; *CASP7*, caspase 7; *CHEK2*, checkpoint kinase 2; *E2F2*, E2F transcription factor 2; *E2F4*, E2F transcription factor 4; *E2F6*, E2F transcription factor 6; GADD45A, growth arrest and DNA-damage-inducible, alpha; GADD45B, growth arrest and DNA-damage-inducible, beta; GADD45G, growth arrest and DNA-damage-inducible, gamma; *HDAC4*, histone deacetylase 4; *HDAC5*, histone deacetylase 5; *PTEN*, phosphatase and tensin homolog; *SIRT3*, sirtuin 3; *SIRT6*, sirtuin 6.

supported by activation of genes involved in cell-cycle arrest and DNA repair following incubation in H_2S. Previous studies have shown that H_2S induces cell-cycle arrest at the G(1) phase in human gingival keratinocytes (11). E2F factors play key roles in the regulation of cell-cycle control and of proapoptotic proteins, like p53 (40). Generally E2F factors are divided into two subclasses: a pro-proliferative class (e.g. E2F2); and a pro-cell cycle exit class (e.g. E2F4 and E2F6) (41). E2F4 is known to play key roles in G1/S transition, S-phase progression and mitosis, whereas E2F6 acts as a repressor of E2F-mediated transcription at the S/G2 phase of the cell cycle (42). Some studies have provided evidence that E2F repressors act downstream of p53 (42–44). After 48 h of incubation, expression of *E2F4* and *E2F6* genes was significantly upregulated in OKSCs. While E2F2 is known to promote cell-cycle progression, overexpression of E2F2 can promote ectopic S-phase entry, ultimately leading to the activation of apoptosis (39). In our experiment, the *E2F2* gene was expressed much more strongly than the other *E2F* factor genes and therefore may contribute to the apoptotic process in OKSCs.

The *PTEN* gene encodes the phosphatase and tensin homolog tumor suppressor protein involved in cell cycle regulation by coordinating G1 arrest and in the apoptotic process by negatively regulating the Akt/PI3K pathway (44). Another important function of PTEN is to protect p53 from MDM2 (murine double minute)-mediated degradation (44). H_2S activated the *PTEN* gene in OKSCs and therefore H_2S may downregulate cell growth and survival. So far, 18 enzymes belonging to the HDAC family have been discovered, each of which plays different roles in cell growth, differentiation, apoptosis or senescence. In our study, the *HDAC4* and *HDAC5* genes were activated following incubation in H_2S. Studies show that HDAC4 inhibits cell-cycle progression in other organs (45). Expression of HDAC4 in keratinocyte stem cells following the cellular stress induced by H_2S inhibits the progression of proliferating OKSCs. HDAC5 appears to act independently from p53 but its overexpression may be involved in initiation of the apoptotic process (46).

Another important event following p53 activation beside apoptosis or cell growth arrest is DNA repair in cells where DNA damage can be corrected.

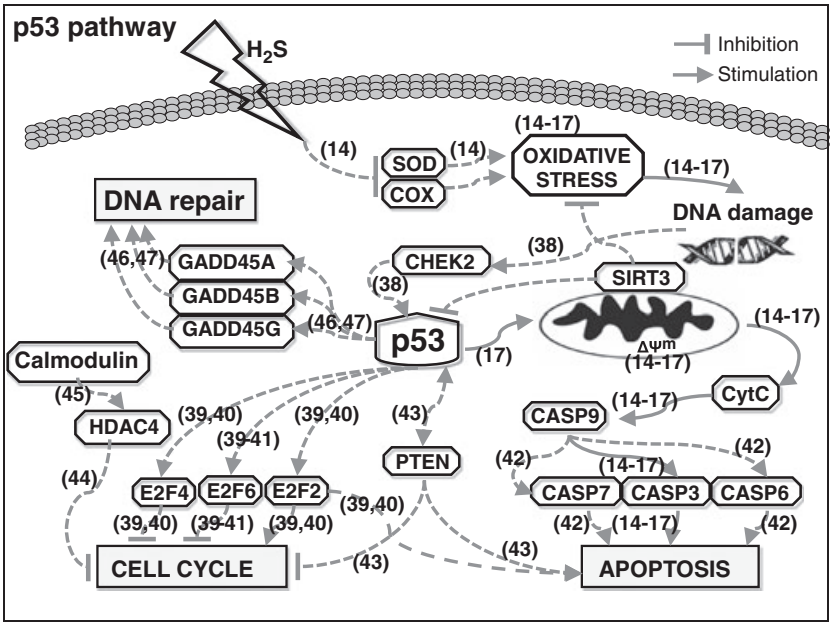

Fig 4. Hydrogen sulfide (H_2S) activates the p53 pathway. Oral keratinocyte stem cells respond by initiating the apoptotic process, cell-cycle arrest and DNA repair mechanisms. The solid line demonstrates the pathways suggested by both ELISA and Human p53 Signaling TaqMan® Array (Applied Biosystems, Foster City, CA, USA), specified for the p53 pathway. The broken line shows the expected pathways based on both quantitative RT-PCR results and previously established pathways. CASP3, caspase-3; CASP6, caspase-6; CASP7, caspase-7; CASP9, caspase-9; CHEK2, serine/threonine-protein kinase Chk2; COX, cyclooxygenase; CytC, cytochrome *c*; E2F2, transcription factor E2F2; E2F4 transcription factor, E2F4; E2F6, transcription factor E2F6; GADD45A, growth arrest and DNA damage-inducible GADD45, alpha; GADD45B, growth arrest and DNA damage-inducible GADD45, beta; GADD45G, growth arrest and DNA damage-inducible GADD45, gamma; HDAC4, histone deacetylase 4; HDAC5, histone deacetylase 5; PTEN, phosphatase and tensin homolog; SOD, superoxide dismutase; SIRT3, sirtuin 3.

The DNA-repair capacity of OKSCs is vital for the normal functioning of the oral epithelial tissue. It is well known that GADD45 is a protein that plays a major role in DNA repair and cell-cycle checkpoints (47,48). Our data showed that all GADD45 genes (*GADD45G*, *GADD45A* and *GADD45B*) were significantly more active when compared with respective controls. This demonstrates that in some OKSCs, p53 also activates the transcription of genes involved in DNA repair. The sirtuin family has important molecular functions in stress regulation and aging (49). In the present study, OKSCs displayed a significant upregulation of *SIRT3* and *SIRT6* genes. The *SIRT3* gene encodes a protein located in the mitochondrial matrix with a key role in cell respiration, decreasing the production of reactive oxygen species and inhibiting p53-regulated growth arrest (50). Recent findings have shown that as a response to oxidative stress, sirtuin 6 is recruited to sites of DNA damage and repairs the DNA double-strand breaks (51). Our data suggested that both sirtuin 6 and sirtuin 3 might act as protective mechanisms developed by OKSCs against the genotoxic effects generated by exposure to H_2S. Finally we determined the p53 pathway activated by H_2S.

VSCs increase the permeability of the gingival crevicular epithelial model (13). Apoptosis is a normal biological event in many tissues, including gingival crevicular epithelia, which maintains a subtle balance between cell loss and production. A disruption of this balance may result in impairment of epithelial, especially OKSC, functions and severely affect the histological architecture and homeostasis in gingival tissues. However, the connection between gingival keratinocyte stem cells and periodontitis has not yet been elucidated. The present study demonstrates that in response to H_2S, the p53 tumor suppressor was activated in OKSCs. The p53 machinery results in protective mechanisms such as DNA repair, cell-cycle inhibition and apoptosis to eliminate cells with nonrepairable DNA damage and to prevent newly divided cells from inheriting chromosomal aberrations (11,52). The above biological functions of OKSCs might prevent malignant formation in the oral cavity (53,54).

Acknowledgements

This research was supported by Grant-In-Aid No. 20390538 from the Japanese Ministry of Education, Culture, Sports, Science and Technology, Tokyo, Japan, the authors report no conflicts of interest related to this study.

References

1. Tonzetich J. Direct gas chromatographic analysis of sulphur compounds in mouth air in man. *Arch Oral Biol* 1971;**16**:587–597.
2. Oho T, Yoshida Y, Shimazaki Y, Yamashita Y, Koga T. Characteristics of patients complaining of halitosis and the usefulness of gas chromatography for diagnosing halitosis. *Oral Surg Oral Med Oral Pathol Oral Radiol Endod* 2001;**91**:531–534.
3. Yaegaki K, Sanada K. Volatile sulfur compounds in mouth air from clinically healthy subjects and patients with periodontitis. *J Periodontal Res* 1992;**27**:233–238.
4. Yaegaki K. Oral malodorous compounds are periodontally pathogenic and carcinogenic. *Jpn Dent Sci Rev* 2008;**44**:100–108.
5. Persson S. Hydrogen sulfide and methyl mercaptan in periodontal pockets. *Oral Microbiol Immunol* 1992;**7**:378–379.
6. Ratkay LG, Waterfield JD, Tonzetich J. Stimulation of enzyme and cytokine production by methyl mercaptan in human gingival fibroblast and monocyte cell cultures. *Arch Oral Biol* 1995;**40**:337–344.

7. Ii H, Imai T, Yaegaki K, Irie K, Ekuni D, Morita G. Oral malodorous compound induces osteoclast differentiation without RANKL. *J Periodontol* 2010; **81**:1691–1697.
8. Irie K, Ekuni D, Tomofugi T, *et al*. Combined effects of hydrogen sulphide and lipopolysaccharide on osteoclast differentiation in rats. *J Periodontol* 2012;**83**:522–527.
9. Yaegaki K. Oral malodor and periodontal disease. In: Rosenberg M, ed. *BAD BREATH: Research Perspectives*. Tel Aviv: Ramat Aviv Pub, 1995: 87–108.
10. Tonzetich J. Effect of volatile sulfur compounds on periodontal tissues and cellular metabolism: an overview. In: van Steenberghe D, Rosenberg M, eds. *Bad Breath, a multidisciplinary approach*. Leuven: Leuven University Press, 1996: 79–91.
11. Takeuchi H, Setoguchi T, Machigashira M, Kanbara K, Izumi Y. Hydrogen sulfide inhibits cell proliferation and induces cell cycle arrest via an elevated p21 Cip1 level in Ca9-22 cells. *J Periodontal Res* 2008;**43**:90–95.
12. Johnson P, Yaegaki K, Tonzetich J. Effect of volatile thiol compounds on protein metabolism by human gingival fibroblasts. *J Periodontal Res* 1992;**27**: 553–561.
13. Ng W, Tonzetich J. Effect of hydrogen sulfide and methyl mercaptan on the permeability of oral mucosa. *J Dent Res* 1984;**63**:994–997.
14. Yaegaki K, Calenic B, Imai T. Induction of apoptosis in human keratinocyte stem cells: the role of hydrogen sulfide. In: Hayat MA, ed. *Stem Cells and Cancer Stem Cells*, Volume 3, Part 6. Dordrecht: Springer, 2012, 371–376.
15. Fujimura M, Calenic B, Yaegaki K, *et al*. Oral malodorous compound activates mitochondrial pathway inducing apoptosis in human gingival fibroblasts. *Clin Oral Investig* 2010;**14**:367–373.
16. Calenic B, Yaegaki K, Murata T, *et al*. Oral malodorous compound triggers mitochondrial-dependent apoptosis and causes genomic DNA damage in human gingival epithelial cells. *J Periodontal Res* 2010;**45**:31–37.
17. Calenic B, Yaegaki K, Kozhuharova A, Imai T. Oral malodorous compound causes oxidative stress and p53-mediated programmed cell death in keratinocyte stem cells. *J Periodontol* 2010;**81**:1317–1323.
18. Riley T, Eduardo Sontag E, Chen P, Levine A. Transcriptional control of human p53-regulated genes. *Nat Rev Mol Cell Biol* 2008;**9**:402–412.
19. Vousden K, Prives C. Blinded by the light: the growing complexity of p53. *Cell* 2009;**137**:413–431.
20. Vousden K, Lane D. p53 in health and disease. *Nat Rev Mol Cell Biol* 2007;**8**:275–283.
21. Calenic B, Ishkitiev N, Yaegaki K, *et al*. Magnetic separation and characterization of keratinocyte stem cell from human gingival. *J Periodontal Res* 2010;**45**:703–708.
22. Livak KJ, Schmittgen TD. Analysis of relative gene expression data using real-time quantitative PCR and the 2(-Delta Delta C(T)). *Methods* 2001;**25**:402–408.
23. Murata T, Yaegaki K, Qian W, *et al*. Hydrogen sulfide induces apoptosis in epithelial cells derived from human gingiva. *J Breath Res* 2008;**2**:017007.
24. Meek DW. Tumor suppression by p53: a role for the DNA damage response? *Nat Rev Cancer* 2009;**10**:714–723.
25. Rufini A, Melino G. Cell death pathology: the war against cancer. *Biochem Biophys Res Commun* 2011;**414**:445–450.
26. Kruse JP, Gu W. Modes of p53 regulation. *Cell* 2009;**137**:609–622.
27. D'Orazi G, Cecchinelli B, Bruno T, *et al*. Homeodomain-interacting protein kinase-2 phosphorylates p53 at Ser 46 and mediates apoptosis. *Nat Cell Biol* 2002;**4**: 11–19.
28. Dorman DC, Moulin FJ, McManus BE, Mahle KC, James RA, Struve MF. Cytochrome oxidase inhibition induced by acute hydrogen sulfide inhalation: correlation with tissue sulfide concentrations in the rat brain, liver, lung, and nasal epithelium. *Toxicol Sci* 2002;**65**: 18–25.
29. Beauchamp RO Jr, Bus JS, Popp JA, Boreiko CJ, Andjelkovich DA. A critical review of the literature on hydrogen sulfide toxicity. *Crit Rev Toxicol* 1984;**13**: 25–97.
30. Truong DH, Eghbal MA, Hindmarsh W, Roth SH, O'Brien PJ. Molecular mechanisms of hydrogen sulfide toxicity. *Drug Metab Rev* 2006;**38**:733–744.
31. Cai J, Wallace DC, Zhivotovsky B, Jones DP. Separation of cytochrome c-dependent caspase activation from thiol-disulfide redox change in cells lacking mitochondrial DNA. *Free Radic Biol Med* 2000;**29**:334–342.
32. Hill MM, Adrain C, Martin SJ. Portrait of a killer: the mitochondrial apoptosome emerges from the shadows. *Mol Interv* 2003;**3**:19–26.
33. Inoue S, Browne G, Melino G, Cohen GM. Ordering of caspases in cells undergoing apoptosis by the intrinsic pathway. *Cell Death Differ* 2009;**16**:1053–1061.
34. Ashkenazi A. Targeting the extrinsic apoptosis pathway in cancer. *Cytokine Growth Factor Rev* 2008;**19**:325–331.
35. Caulín C, Salvesen GS, Oshima RG. Caspase cleavage of keratin 18 and reorganization of intermediate filaments during epithelial cell apoptosis. *J Cell Biol* 1997;**138**:1379–1394.
36. Lakhani SA, Masud A, Kuida K, *et al*. Caspases 3 and 7: key mediators of mitochondrial events of apoptosis. *Science* 2006;**311**:847–851.
37. Martinon F, Tschopp J. Inflammatory caspases and inflammasomes: master switches of inflammation. *Cell Death Differ* 2007;**14**:10–22.
38. Hitomi J, Katayama T, Eguchi Y, *et al*. Involvement of caspase-4 in endoplasmic reticulum stress-induced apoptosis and Abeta-induced cell death. *J Cell Biol* 2004;**165**:347–356.
39. Chehab NH, Malikzay A, Appel M, Halazonetis TD. Chk2/hCds1 functions as a DNA damage checkpoint in G1 by stabilizing p53. *Genes Dev* 2000;**14**:278–288.
40. DeGregori J, Johnson DG. Distinct and overlapping roles for E2F family members in transcription, proliferation and apoptosis. *Curr Mol Med* 2006;**6**:739–748.
41. Trimarchi JM, Lees JA. Sibling rivalry in the E2F family. *Nat Rev Mol Cell Biol* 2002;**3**:11–20.
42. Giangrande PH, Zhu W, Schlisio S, *et al*. A role for E2F6 in distinguishing G1/S- and G2/M-specific transcription. *Genes Dev* 2004;**18**:2941–2951.
43. Jung EM, An BS, Choi KC, Jeung EB. Apoptosis- and endoplasmic reticulum stress-related genes were regulated by estrogen and progesterone in the uteri of calbindin-D(9k) and -D(28k) knockout mice. *J Cell Biochem* 2012;**113**:194–203.
44. Chu EC, Tarnawski AS. PTEN regulatory functions in tumor suppression and cell biology. *Med Sci Monit* 2004;**10**:235–241.
45. Majdzadeh N, Wang L, Morrison BE, Bassel-Duby R, Olson EN, D'Mello SR. HDAC4 inhibits cell-cycle progression and protects neurons from cell death. *Dev Neurobiol* 2008;**68**:1076–1092.
46. Usui T, Okada M, Hara Y, Yamawaki H. Exploring calmodulin related proteins, which mediate development of hypertension, in vascular tissues of spontaneous hypertensive rats. *Biochem Biophys Res Commun* 2011;**405**:47–51.
47. Liebermann DA, Hoffman B. Gadd45 in stress signaling. *J Mol Signal* 2008;**3**:15.
48. Rosemary Siafakas A, Richardson DR. Growth arrest and DNA damage-45 alpha (GADD45alpha). *Int J Biochem Cell Biol* 2009;**41**:986–989.
49. Milne JC, Denu JM. The Sirtuin family: therapeutic targets to treat diseases of aging. *Curr Opin Chem Biol* 2008;**12**:11–17.
50. Kawamura Y, Uchijima Y, Horike N, *et al*. Sirt3 protects in vitro–fertilized mouse preimplantation embryos against oxidative stress–induced p53-mediated

developmental arrest. *J Clin Invest* 2010;**120**:2817–2828.
51. Taira N, Yoshida K. Post-translational modifications of p53 tumor suppressor: determinants of its functional targets. *Histol Histopathol* 2012;**27**:437–443.
52. Mao Z, Hine C, Tian X, *et al*. SIRT6 promotes DNA repair under stress by activating PARP1. *Science* 2011;**332**:1443–1446.
53. Levi PA Jr, Kim DM, Harsfield SL, Jacobson ER. Squamous cell carcinoma presenting as an endodontic-periodontic lesion. *J Periodontol* 2005;**76**:1798–1804.
54. Halazonetis TD, Gorgoulis VG, Bartek J. An oncogene-induced DNA damage model for cancer development. *Science* 2008;**319**:1352–1355.